

Strange quark suppression and strange hadron production in pp collisions at RHIC and LHC

Hai-Yan Long and Sheng-Qin Feng*

Dept. of Physics, College of Science, China Three Gorges Univ., Yichang 443002, China

Dai-Mei Zhou

Institute of Particle Physics, Huazhong Normal University, Wuhan 430082, China

Yu-Liang Yan and Hai-Liang Ma

China Institute of Atomic Energy, P. O. Box 275 (18), Beijing 102413, China

Ben-Hao Sa†

China Institute of Atomic Energy, P. O. Box 275 (18), Beijing 102413, China

*Institute of Particle Physics, Huazhong Normal University, Wuhan 430082, China and
CCAST (World Laboratory), P. O. Box 8730, Beijing 100080, China*

The parton and hadron cascade model PACIAE based on PYTHIA is utilized to systematically investigate strange particle production in pp collisions at the RHIC and LHC energies. Globally speaking, the PACIAE results of the strange particle rapidity density at mid-rapidity and the transverse momentum distribution are better than PYTHIA (default) in comparing with STAR and ALICE experimental data. This may represent the importance of the parton and hadron rescatterings, as well as the reduction mechanism of strange quark suppression, added in the PACIAE model. The K/π ratios as a function of reaction energy in pp collisions from SPS to LHC energies are also analyzed in this paper.

Keywords: strange particle, rapidity distribution, transverse momentum distribution, PYTHIA model, PACIAE model.

PACS numbers: 25.75.Dw, 24.10.Lx

I. INTRODUCTION

Strange particle production is a powerful probe into the hadronic interaction and the hadronization process in pp and heavy ion collisions at relativistic energies. The strangeness enhancement in relativistic nucleus-nucleus collisions relative to pp collisions at the same energy has been proposed as a signature of the Quark-Gluon Plasma (QGP) formation in the relativistic heavy ion collisions [1]. This is based on the principle that the threshold energy of strange particle production in Quark-Gluon Matter (QGM) is higher than that in hadronic matter. Unfortunately, the QGM has not yet been confirmed to be unique explanation of strangeness enhancement.

The Large Hadron Collider (LHC) at CERN opens a new era in the investigation of nucleus-nucleus collisions at relativistic energy. It has established a new platform to study the properties of QCD matter (QGM) [2, 3]. Strangeness production is one of the most important research topics in the relativistic nuclear collisions at the LHC. Recently, the ALICE collaboration reported their data of strange particle production in pp collisions at $\sqrt{s} = 0.9$ TeV [4, 5]. This introduces a new energy regime

in the research of strangeness production and the possibility to compare with the previous measurements in pp collisions at $\sqrt{s}=200$ GeV [6].

In the LUND string fragmentation scheme [7], the suppression of s quark pair production compared with u (d) pair production (the parameter $parj(2)$ in PYTHIA or λ denoted later) was assumed to be fixed. However, later experiments [8] have shown that this suppression decreases with increasing reaction energy. In Ref. [9], the reduction mechanism of the strange quark suppression has been introduced in the LUCIAE model. By this mechanism, they described the strangeness enhancement in pp, p+A, and A+A collisions at SPS energies successfully [9, 10]. LUCIAE is a hadron cascade model based on FRITIOF [11] with the firecracker model and hadronic rescattering added [12].

In this paper, the reduction mechanism of the strange quark suppression was introduced in the parton and hadron cascade model PACIAE [13] and denoted as the modified PACIAE model to distinguish it from the default one. The modified PACIAE model was then used to systematically investigate the strange particle production in pp collisions at the RHIC and LHC energies.

This paper is organized as follows. In Sec. II, we give a brief review the PACIAE model [13] and the reduction mechanism of strangeness quark suppression [9]. In Sec. III, we use the modified parton and hadron cascade model PACIAE based on PYTHIA [14] to analyze sys-

*Electronic address: fengsq@ctgu.edu.cn

†Electronic address: sabh@ciae.ac.cn

tematically the strangeness production in pp collisions at RHIC and LHC energies [4–6]. The K/π ratio as a function of reaction energy in pp collisions at relativistic energies from SPS to LHC was also investigated in Sec.III. Section IV gives a summary and conclusion.

II. MODELS

PACIAE [13] is a parton and hadron cascade model based on PYTHIA [14] which is a model for high energy hadron-hadron (hh) collisions at the hadronic level. In the PYTHIA model, a pp collision is decomposed into parton-parton collisions. The hard parton-parton interaction is described by the lowest leading order perturbative QCD (LO-pQCD). The soft parton-parton collision, a non-perturbative phenomenon, is considered empirically. The initial- and final-state QCD radiations, as well as the multiparton interactions, are considered. Therefore the consequence of a pp collision is a parton multijet configuration composed of quarks (anti-quarks), di-quarks (anti-diquarks) and gluons, along with a few hadronic remnants. After that, the string construction and fragmentation (hadronization) are performed to obtain a hadronic final state for a pp collision.

For the pp collision, the PACIAE model is different from PYTHIA in the addition of the parton initiation stage, the parton rescattering before hadronization, and the hadron rescattering after hadronization. Thus, the PACIAE model consists of the parton initiation, parton evolution (rescattering), hadronization, and hadron evolution (rescattering) four stages.

In order to create the parton initiation stage for a pp collision, the string fragmentation is switched off temporarily in PACIAE. The di-quarks (anti-diquarks) are broken up. Then the partonic initial state is obtained in the PACIAE model, instead of the hadronic final state in PYTHIA. This is just QGM formed in the parton initiation stage of a pp collision.

The rescattering among partons in QGM is considered by the $2 \rightarrow 2$ LO pQCD parton-parton cross sections [15]. By integrating this differential cross section properly, the total cross section is obtained. With the differential and total cross sections, parton rescattering is performed by the Monte Carlo method.

In the hadronization stage, the QGM formed after parton rescattering is hadronized by the LUND string fragmentation regime [7, 14] or the Monte Carlo coalescence model proposed in [13]. The LUND string fragmentation is used in this paper.

The hadronic rescattering is modeled with the usual two body elastic and/or inelastic collisions [12], until the hh collision pairs are exhausted (hadronic freeze-out). The rescatterings among π , K , p , n , $\rho(\omega)$, Δ , Λ , Σ , Ξ , J/Ψ and their antiparticles are considered for the moment.

In the PYTHIA model [14], it is assumed that the $q\bar{q}$ pair with quark mass m and transverse momentum p_T

is first created quantum mechanically at one point and then tunnel out to the classically allowed region. This tunnelling probability is calculated

$$\exp\left(-\frac{\pi m^2}{\kappa}\right) \exp\left(-\frac{\pi p_T^2}{\kappa}\right), \quad (1)$$

where the string tension is assumed to be a constant of $\kappa \approx 1 \text{ GeV/fm} \approx 0.2 \text{ GeV}^2$ [7, 14]. This probability implies a suppression of strange (heavy) quark production: $u : d : s : c \approx 1 : 1 : 0.3 : 10^{-11}$. Therefore the charm and heavier quarks are not expected to be produced in the soft string fragmentation process but only in the hard process or as a part of the initial- and final-state QCD radiations.

A reduction mechanism of strange quark suppression was introduced in [9] by assuming that the effective string tension increased with increasing reaction energy. Hence the strange (heavy) quark production increased with increasing reaction energy. It was further assumed in [9] that the effective string tension variation with reaction energy could be considered by the effective string tension as a function of the number and the hardening of gluons in a single string as follows:

$$\kappa^{eff} = \kappa_0 (1 - \xi)^{-\alpha}, \quad (2)$$

$$\xi = \frac{\ln\left(\frac{k_{Tmax}^2}{s_0}\right)}{\ln\left(\frac{s}{s_0}\right) + \sum_{j=2}^{n-1} \ln\left(\frac{k_{Tj}^2}{s_0}\right)}, \quad (3)$$

where κ_0 is the string tension of a pure $q\bar{q}$ string, assumed to be $\sim 1 \text{ GeV/fm}$. Here it should be mentioned that the above Eq. (3) represents the deviation scale of the multigluon string from the pure string. The gluons in a multigluon string are ordered from 2 to $n-1$, because of the quark and antiquark on both ends of string with index 1 and n , respectively. k_{Tj}^2 (k_{Tmax}) is the transverse momentum of gluon j with $k_{Tj} > s_0$ (gluon largest transverse momentum). The parameters $\alpha=3.5 \text{ GeV}$ and $\sqrt{s_0}=0.8 \text{ GeV}$ were determined by fitting the hh collision data [9].

The strange quark suppression factor λ (i.e. $parj(2)$ in PYTHIA) and the width σ ($parj(21)$ in PYTHIA) of the Gaussian p_x and p_y transverse momentum distributions of the primary hadrons, in a string with effective string tension κ_1^{eff} , are denoted by λ_1 and σ_1 , respectively. These two quantities in a string with effective string tension κ_2^{eff} , λ_2 and σ_2 , can be calculated by Eq. (1)

$$\lambda_2 = \lambda_1 \frac{\kappa_1^{eff}}{\kappa_2^{eff}}, \quad (4)$$

$$\sigma_2 = \sigma_1 \left(\frac{\kappa_2^{eff}}{\kappa_1^{eff}}\right)^{1/2}. \quad (5)$$

In the PYTHIA model there are parameters $parj(1)$ and $parj(3)$ related to strangeness production, besides $parj(2)$ and $parj(21)$. $parj(1)$ is the suppression of diquark-antidiquark pair production relative to the quark-antiquark pair production. $parj(3)$ refers to the extra suppression of strange diquark production relative to the normal suppression of strange quark production. For double strange particle (strange baryon) production, $parj(1)$ and $parj(3)$ have to be considered as well. It is not hard to prove that the Eq. (4) is also valid for $parj(1)$ and $parj(3)$.

III. CALCULATIONS AND RESULTS

The reduction mechanism of the strange quark suppression has been included in the PACIAE model. One might first tune the parameters $parj(1)$, $parj(2)$, and $parj(3)$ to fit the strangeness production data in a given nuclear collision system at a given energy. The resulting $parj(1)$, $parj(2)$, and $parj(3)$ and the effective string tension can be used to predict the strangeness production in the same reaction system at different energies, even in different reaction systems.

As we aimed at the physics behind the strange particle production and not at the reproduction of experimental data, we kept all model parameters at their default values. However, the higher order and non-perturbative correction factor in parton-parton interaction, K , was assumed to be 3.

We then first globally tuned the parameters $parj(1)$, $parj(2)$, and $parj(3)$ in default PACIAE simulations to fit the strangeness production data from NSD (non single diffractive) pp collisions at $\sqrt{s}=200$ GeV [6]. The results are shown in Tab. I along with the results from default PYTHIA simulations. From this table, we find that the STAR data are better described by default PACIAE model rather than by the default PYTHIA model.

The strange particle transverse momentum spectra in the NSD pp collisions at $\sqrt{s}=200$ GeV calculated by the default PACIAE and default PYTHIA are shown in Fig. 1. The corresponding STAR data [6] are also given. The panels (a), (b), and (c) are for K_s^0 , Λ , and Ξ^- , respectively. These results indicate that, globally speaking, the strange particle p_T spectrum is better described by the default PACIAE rather than the default PYTHIA model. Here, the role of parton and hadron rescatterings is also not negligible.

The fitted parameters of $parj(1)=0.18$, $parj(2)=0.4$, and $parj(3)=0.5$ as well as the calculated $\kappa^{eff}=1.387$ were then used to calculate the strange particle production in INEL (inelastic) pp collisions at $\sqrt{s}=900$ GeV by the modified PACIAE model. The resulting strange particle rapidity densities at mid-rapidity were compared with the ALICE data [4] as well as the results of default PYTHIA in Tab. II. One sees in this table that the ALICE data are better reproduced by modified PACIAE, rather than the default PYTHIA model. The effects of

the reduction mechanism of strange quark suppression and the parton and hadron rescatterings may be all important which has to be separately studied.

We present the strange particle transverse momentum distributions in INEL pp collisions at $\sqrt{s}=900$ GeV calculated by the modified PACIAE and default PYTHIA models in Fig. 2. The corresponding ALICE data [4] are also given. The panels (a), (b), (c), and (d) are for K_s^0 , ϕ , Λ , and $\Xi^-+\Xi^+$, respectively. One sees in Fig. 2 that the modified PACIAE results fit well with the ALICE data for the light strange particle K_s^0 . However, for the ϕ meson and the heavy strange baryons (Λ and $\Xi^-+\Xi^+$) the modified PACIAE model overestimates the data in the $p_T > 1$ GeV/c region. This may be because we only used the default PACIAE to tune the parameters to the data of strange particle rapidity densities at mid-rapidity in $\sqrt{s}=200$ GeV pp collisions [6]. In this sense, the transverse momentum distribution is calculated parameter free. Therefore, even if the calculated strange particle rapidity densities at mid-rapidity are close to the data (cf. Tab. I and Tab. II), the calculated transverse momentum distribution may not be closely similar to the data. Thus, the calculated transverse momentum distribution is softer than the data in the $p_T < 1$ GeV/c region, but harder in the $p_T > 1$ GeV/c region. It might also be possible that the reduction mechanism of strange quark suppression is not so suitable for the heavy strange baryons. Therefore, the role played by the reduction mechanism of strange quark suppression and the parton and hadron rescatterings are worthy to be separately studied in the next investigations.

Similarly, the transverse momentum distribution of K_s^0 , Λ , and Ξ^- in INEL pp collisions at $\sqrt{s}=2.36, 7$, and 14 TeV were predicted by the modified PACIAE model and given in Fig. 3. These results are prepared to compare with the future experimental measurements at the LHC.

In [5, 16], the experimental kaon to pion ratios in pp and/or $p\bar{p}$ collisions at different reaction energies from SPS to LHC were plotted in a K/π versus \sqrt{s} figure, although their experimental details in the measured observable (K^+/π^+ , or $(K^+ + K^-)/(\pi^+ + \pi^-)$, or K^0/π^0) and the rapidity acceptance were different from each other. These experimental ratios are copied in Fig. 4. In this figure, NA49, STAR, ALICE, E735, and UA5 data were taken from [17], [18], [5, 16], [19], and [20], respectively. In [5, 16], it was concluded that the “ratio shows a slight increase from $\sqrt{s}=200$ GeV ($K/\pi = 0.103 \pm 0.008$) to $\sqrt{s}=900$ GeV ($K/\pi = 0.123 \pm 0.004 \pm 0.010$), yet consistent within the error bars. The results at 7 TeV will show whether the K/π ratio keeps rising slowly as a function of \sqrt{s} or saturates.” To respond to this challenge the $(K^+ + K^-)/(\pi^+ + \pi^-)$ ratio was extracted from the above PACIAE model simulations for pp collisions at $\sqrt{s}=0.2, 0.9, 2.36, 7$, and 14 TeV and given in Fig. 4 by red triangles. In addition, the default PACIAE and PYTHIA models were used to calculate the NA49 $(K^+ + K^-)/(\pi^+ + \pi^-)$ ratio in pp collisions at 158

GeV/c beam momentum. The model parameters employed in these calculations were the same as the ones used in the above simulations, except $K=1$ was assumed because of the low energy.

We find in Fig. 4 that the PACIAE results at $\sqrt{s}=17.2$, 200 and 900 GeV agree with the NA49, STAR, and ALICE data, respectively, within error. Together with the PACIAE results at $\sqrt{s}=2.36$, 7, and 14 TeV, it seems to indicate that the K/π ratio as a function of \sqrt{s} first increases slightly from $\sqrt{s}=0.2$ to 0.9 TeV and then saturates. Of course, this rough trend of the K^+/π^+ ratio as a function of \sqrt{s} in pp reactions has to be further studied in detail both experimentally and theoretically.

IV. CONCLUSIONS

In summary, we used the parton and hadron cascade model PACIAE with the reduction mechanism of the strange quark suppression and default PYTHIA models to systematically investigate the production of strange particles in NSD and INEL pp collisions at $\sqrt{s}=200$ GeV and $\sqrt{s}=0.9$, 2.36, 7, and 14 TeV, respectively. The calculated strangeness transverse momentum distributions in NSD pp collisions at $\sqrt{s}=200$ GeV compare well with the STAR data [6] and PACIAE is globally better than the default PYTHIA model. We also compared the calculated strange particle rapidity densities at mid-rapidity and transverse momentum distributions in INEL pp collisions at $\sqrt{s}=0.9$ TeV with the corresponding ALICE data [4]. The agreement between theory and experiment is good and the PACIAE is globally better than the default PYTHIA model. This may indicate the significant effect of the parton and hadron rescatterings, as well as the reduction mechanism of strange quark suppression. These effects are worth investigating separately.

The K/π ratios calculated by PACIAE in NSD pp colli-

sions at $\sqrt{s}=0.2$ TeV and in INEL pp collisions at $\sqrt{s}=0.9$ TeV agree with the corresponding STAR [18] and ALICE data [5, 16], respectively, within error. The PACIAE model result in pp collisions at 158 GeV/c beam momentum is also comparable with NA49 data [17]. The rough trend of the K/π ratio as function of \sqrt{s} shown in Fig. 4 seems to be first increasing moderately, then slightly, and finally saturating. This trend has to be studied in detail both experimentally and theoretically.

Just before the submission of this paper, we read the paper of [21] and knew that the CMS measured “ p_T distributions are found to differ substantially from PYTHIA results and the production rates exceed the predictions by up to a factor of three.” Note, here PYTHIA refers to a variety of PYTHIA tunes quoted in [21]. We use the modified PACIAE model to calculate the corresponding values. The calculated $dN/dy|_{y \approx 0} = 0.238$, 0.102, and 0.0113 for K_s^0 , Λ , and Ξ^- compare well with the CMS data of $0.205 \pm 0.001 \pm 0.015$, $0.108 \pm 0.001 \pm 0.012$, $0.011 \pm 0.001 \pm 0.001$ [21] in NSD pp collisions at $\sqrt{s}=0.9$ TeV, respectively. Similarly, the PACIAE results of 0.403, 0.166, and 0.0183 compare well with the data of $0.346 \pm 0.001 \pm 0.025$, $0.189 \pm 0.001 \pm 0.022$, and $0.021 \pm 0.001 \pm 0.003$, respectively, in NSD pp collisions at $\sqrt{s}=7$ TeV. The calculated rapidity and transverse momentum distributions are compared with the CMS data [21] in Fig. 5. The agreement is better than the PYTHIA tunes quoted in [21].

Acknowledgments

Financial support from the National Science Foundation of China (10975091, 11075217, 11047142, and 10975062) is acknowledged. BHS would like to thank Dr. James Ketudat Cairns for help improving the English.

-
- [1] J. Rafelski, Phys. Rep. **88**, 331 (1982).
 - [2] V. T. Pop, *et al.*, Phys. Rev. C **83**, 024902 (2011).
 - [3] N. Armesto, *et al.*, J. Phys. G **35**, 054001 (2008).
 - [4] K. Admodt *et al.*, ALICE Collaboration, Eur. Phys. J. C **71**, 1594, (2011).
 - [5] H. Oeschler, ALICE Collaboration, arXiv:1102.2745v1.
 - [6] B. I. Abelev *et al.*, STAR Collaboration, Phys. Rev. C **75**, 064901 (2004).
 - [7] B. Andersson, G. Gustafson, G. Ingelman and T. Sjöstrand, Phys. Rep. **97**, 31 (1983).
 - [8] G. Bocquet, *et al.*, UA1 Collaboration, Phys. Lett. B **366**, 447 (1996).
 - [9] An Tai and Ben-Hao Sa, Phys. Lett. B **409**, 394 (1997).
 - [10] An Tai and Ben-Hao Sa, Phys. Rev. C **57**, 261 (1998).
 - [11] H. Pi, Comput. Phys. Commun. **71**, 173 (1992).
 - [12] Ben-Hao Sa and Tai An, Comput. Phys. Commun. **90**, 121 (1995); Tai An and Ben-Hao Sa, Comput. Phys. Commun. **116**, 353 (1999).
 - [13] Most recent references: Ben-Hao Sa, Dai-Mei Zhou, Bao-Guo Dong, Yu-Liang Yan, Hai-Liang Ma, and Xiao-Mei Li, J. Phys. G: Nucl. Part. Phys. **36**, 025007 (2009); Yu-Liang Yan, Dai-Mei Zhou, Bao-Guo Dong, Xiao-Mei Li, Hai-Liang Ma, and Ben-Hao Sa, Phys. Rev. C **79**, 054902 (2009); Ben-Hao Sa, Dai-Mei Zhou, Yu-Liang Yan, Xiao-Mei Li, Sheng-Qin Feng, Bao-Guo Dong, and Xu Cai, arXiv:1104.1238v1.
 - [14] T. Sjöstrand, S. Mrenna, and P. Skands, J. High Energy Phys. **05**, (2006) 026.
 - [15] B. L. Combridge, J. Kripfgang, J. Ranft, Phys. Lett. B **70**, 234 (1977).
 - [16] K. Admodt, *et al.*, ALICE Collaboration, Eur. Phys. J. C **71**, 1655 (2011).
 - [17] C. Alt, *et al.* NA49 Collaboration, Eur. Phys. J. C **45**, 343 (2006); T. Anticic, *et al.*, NA49 Collaboration, Eur. Phys. J. C **68**, 1 (2010).
 - [18] B. I. Abelev, *et al.*, STAR Collaboration, Phys. Rev. C **79** 034909 (2009).
 - [19] T. Alexopoulos, *et al.*, E735 Collaboration, Phys. Rev. D

- 48**, 984 (1993).
- [20] G. J. Alner, *et al.*, UA5 Collaboration, Nucl. Phys. B **258**, 505 (1985).
- [21] CMS Collaboration, JHEP 05, 064 (2011).

TABLE I: Strange particles rapidity densities at mid-rapidity ($|y| < 0.5$) in NSD pp collisions at $\sqrt{s}=200$ GeV. The STAR data were taken from [6].

	STAR	PACIAE	PYTHIA
K_s^0	0.134 ± 0.011	0.127	0.107
K^+	0.140 ± 0.01	0.135	0.112
K^-	0.137 ± 0.009	0.123	0.104
Λ	0.0385 ± 0.0036	0.0360	0.0163
$\bar{\Lambda}$	0.0351 ± 0.0033	0.0350	0.0163
Ξ^-	0.0026 ± 0.00092	0.00373	0.00106
Ξ^+	0.0029 ± 0.001	0.00364	0.00099
$\Omega^- + \bar{\Omega}^+$	0.00034 ± 0.00019	0.00026	0.00005

TABLE II: Strange particles rapidity densities at mid-rapidity in INEL pp collisions at $\sqrt{s}=900$ GeV. The ALICE data were taken from [4].

	$ y $	$p_T(GeV/c)$	ALICE	PACIAE	PYTHIA
K_s^0	< 0.75	[0.2-3.0]	0.184 ± 0.0063	0.15	0.172
Φ	< 0.60	[0.7-3.0]	0.021 ± 0.005	0.019	0.0134
Λ	< 0.75	[0.6-3.5]	0.048 ± 0.00412	0.043	0.0227
$\bar{\Lambda}$	< 0.75	[0.6-3.5]	0.047 ± 0.00539	0.043	0.0230
$\Xi^- + \Xi^+$	< 0.80	[0.6-3.0]	0.0101 ± 0.00219	0.0086	0.00354

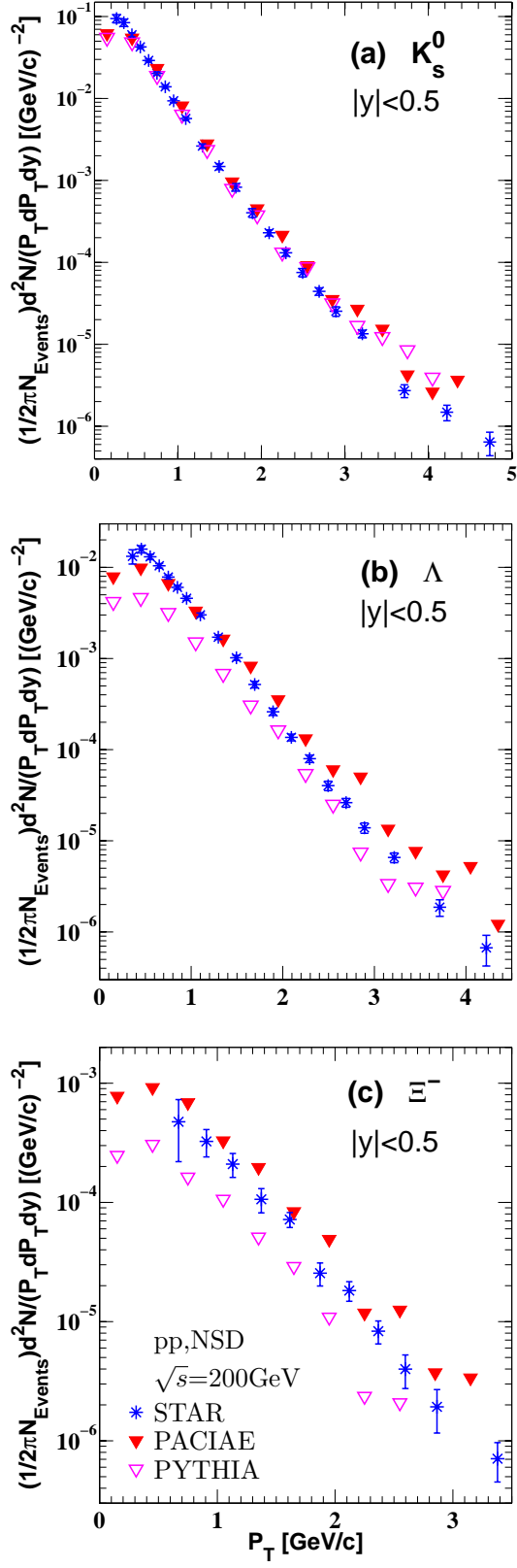


FIG. 1: (Color online) Transverse momentum distribution of strange particles in NSD pp collisions at $\sqrt{s}=200 \text{ GeV}$. Panels (a), (b) and (c) are for K_s^0 , Λ , and Ξ^- , respectively. The STAR data were taken from [6].

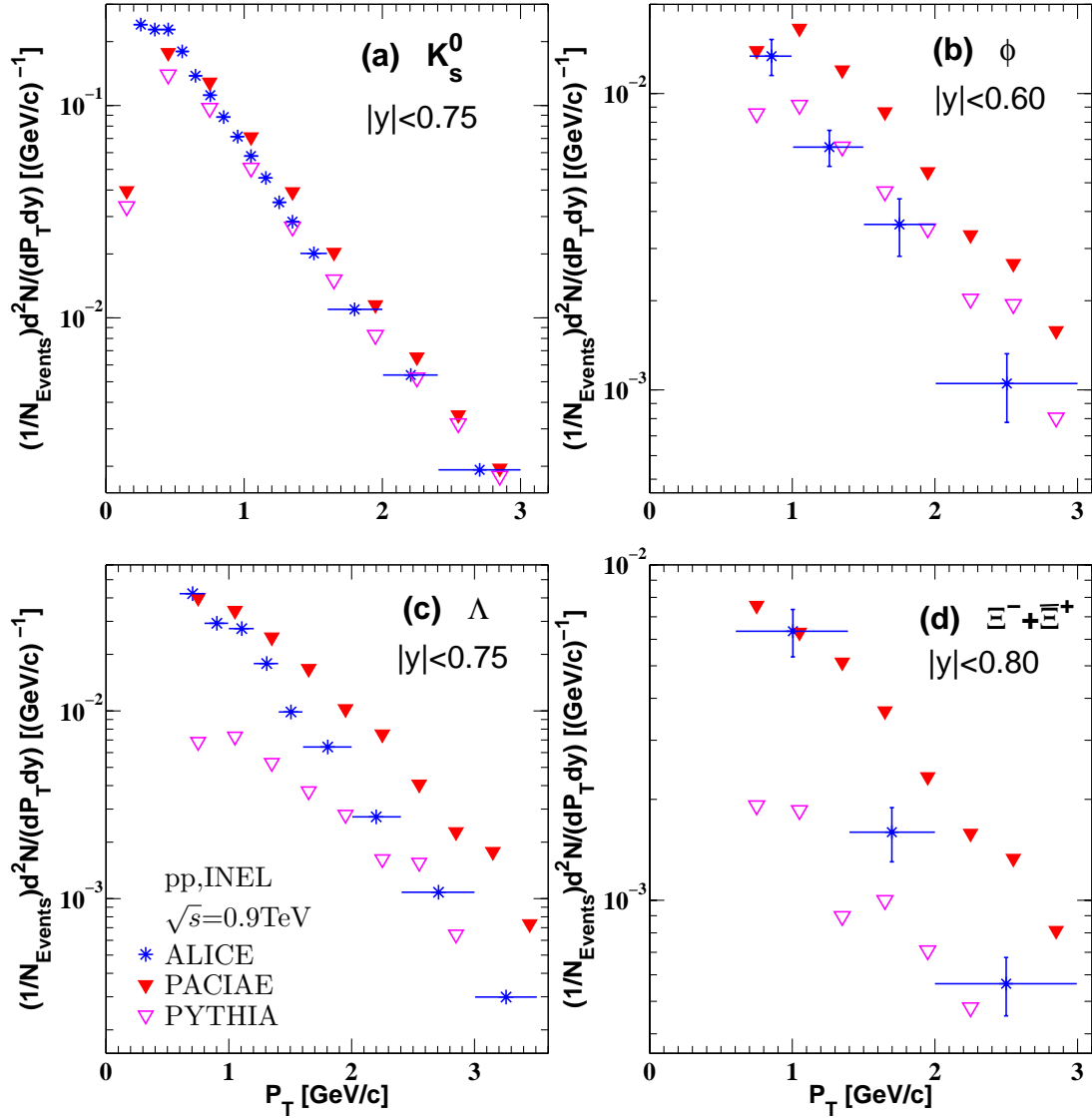


FIG. 2: (Color online) Transverse momentum distributions of strange particles in INEL pp collisions at $\sqrt{s}=900$ GeV. Panels (a), (b), (c), and (d) are for K_s^0 , ϕ , Λ , and $\Xi^- + \Xi^+$, respectively. The ALICE data were taken from [4]

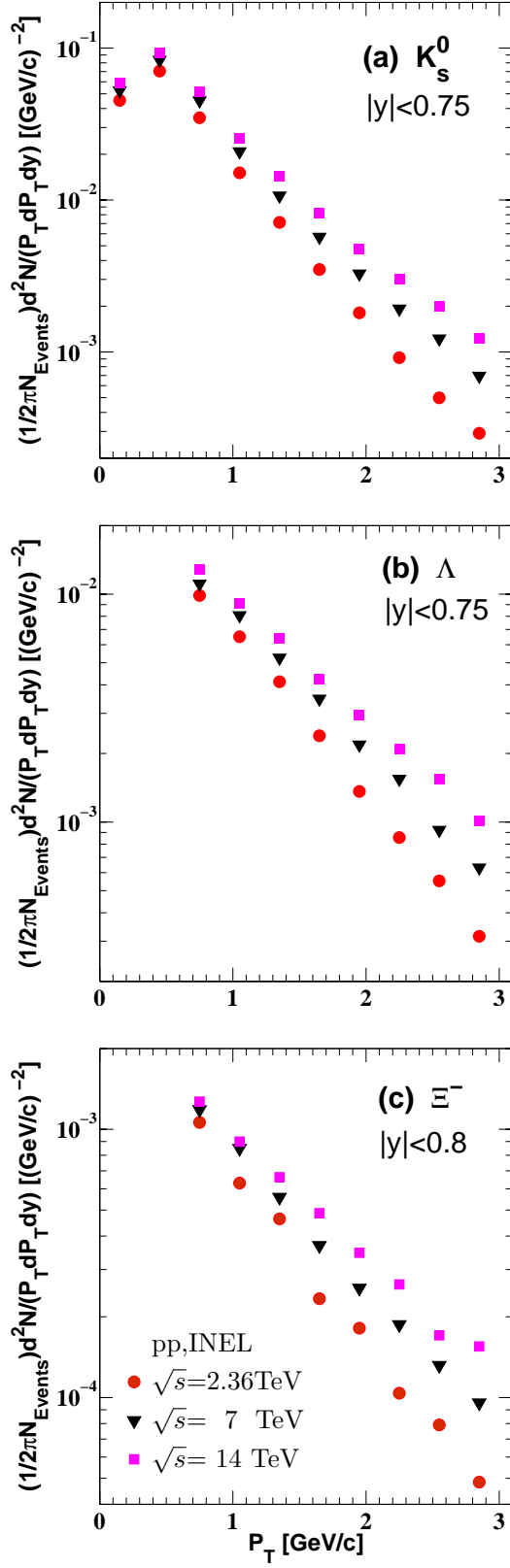


FIG. 3: (Color online) Transverse momentum distributions of strange particles in INEL pp collisions at $\sqrt{s}=2.36, 7$, and 14 TeV calculated by PACIAE. Panels (a), (b), and (c) are for K_s^0 ($|y| < 0.75$), Λ ($|y| < 0.75$), and Ξ^- ($|y| < 0.80$), respectively.

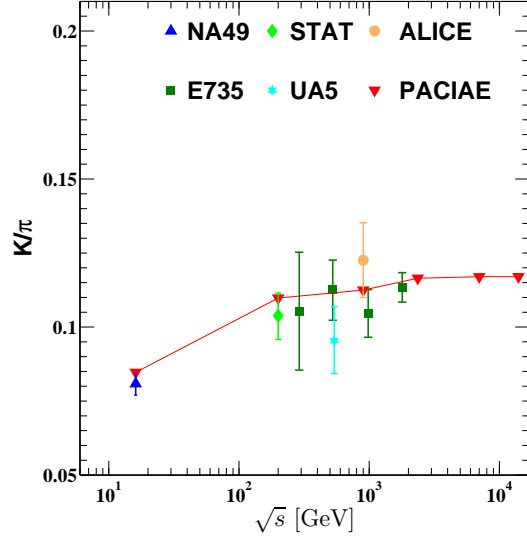


FIG. 4: (Color online) K/π ratio as a function of \sqrt{s} in pp collisions at relativistic energies.

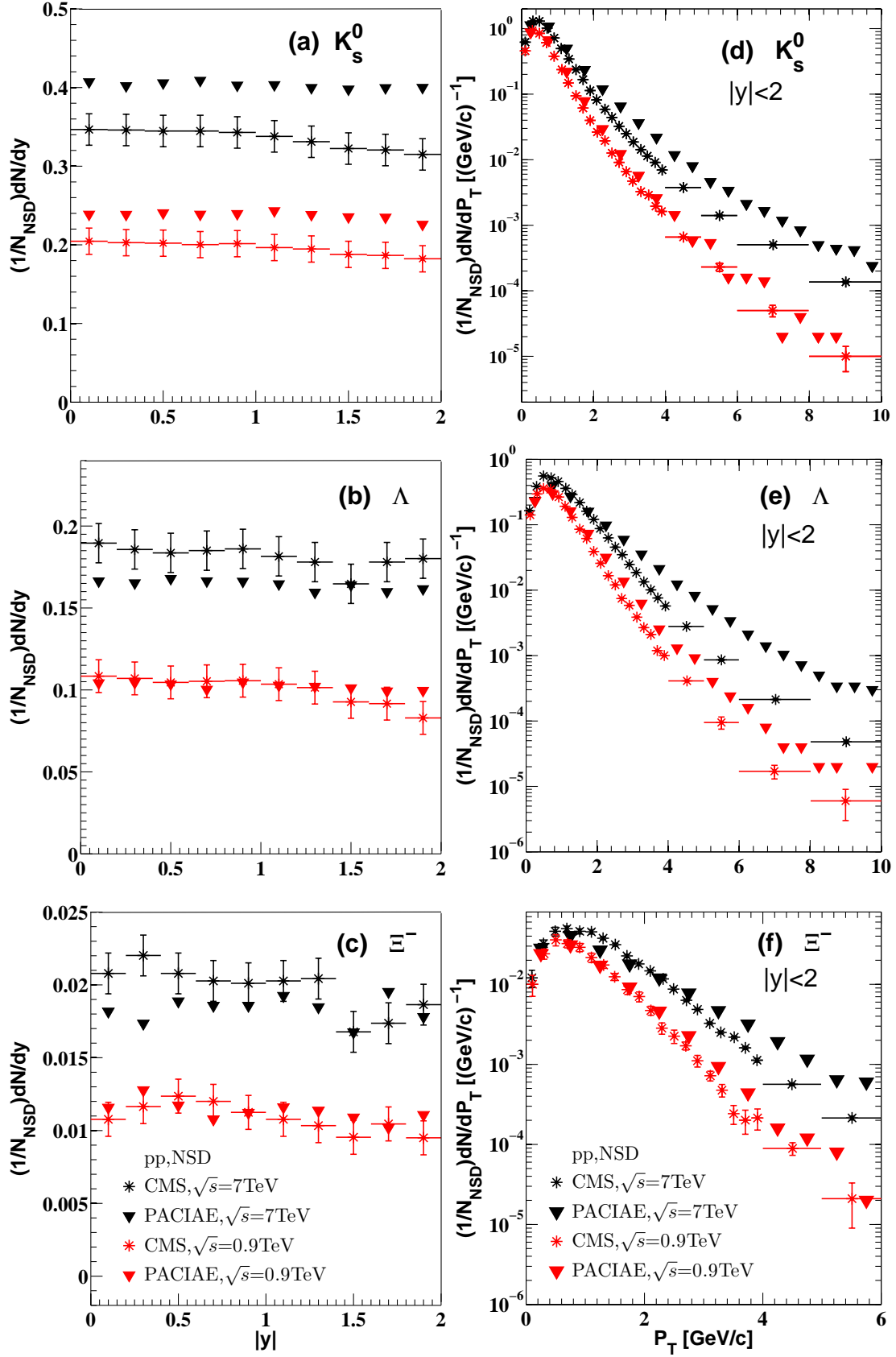


FIG. 5: (Color online) Left panel: the strange particle rapidity distributions for K_s^0 (a), Λ (b), and Ξ^- (c) in NSD pp collisions at $\sqrt{s}=0.9$ and 7 TeV. Right panel: the transverse momentum distributions for K_s^0 (d), Λ (e), and Ξ^- (f). The CMS data were taken from [21].